

# Fabrication of high-brightness silicon vacancy color-center ensembles in 4H-SiC via MeV particles

Cite as: Appl. Phys. Lett. **127**, 064002 (2025); doi: [10.1063/5.0288542](https://doi.org/10.1063/5.0288542)

Submitted: 1 July 2025 · Accepted: 26 July 2025 ·

Published Online: 12 August 2025



Shang Tian,<sup>1</sup> Huaqing Huang,<sup>1</sup> Haozheng Guo,<sup>1</sup> Jianhan Sun,<sup>1</sup> Yulan Liang,<sup>1</sup> Yewei Song,<sup>1</sup> Yunbiao Zhao,<sup>1</sup> Yuan Gao,<sup>1</sup> Lin Lin,<sup>1</sup> Senlin Huang,<sup>1</sup> Wenjun Ma,<sup>1</sup> and Jianming Xue<sup>1,2,a)</sup>

## AFFILIATIONS

<sup>1</sup>State Key Laboratory of Nuclear Physics and Technology, School of Physics, Peking University, Beijing 100871, China

<sup>2</sup>CAPT and HEDPS, College of Engineering, Peking University, Beijing 100871, China

<sup>a)</sup>Author to whom correspondence should be addressed: [jmxue@pku.edu.cn](mailto:jmxue@pku.edu.cn)

## ABSTRACT

The silicon vacancy ( $V_{Si}^-$ ) color centers in 4H-SiC are promising solid-state spin defects for quantum sensing applications, featuring long room-temperature coherence times, near-infrared photoluminescence, and an optically controllable spin–photon interface. However, it is essential to achieve high-brightness silicon vacancy color-center ensembles by different irradiations for efficient signal detection and high-fidelity quantum sensing. In this work, we conducted irradiation experiments of MeV electrons, protons, and laser-driven ions to investigate the influence of irradiation parameters on the fabrication of  $V_{Si}^-$  center ensembles, confirming the vital roles of crystal damage densities in the production yield of  $V_{Si}^-$  centers. Furthermore, the hot irradiation experiments reveal that irradiation at optimized temperatures can enhance the production yield of  $V_{Si}^-$  centers and break the inherent limitation of radiation-induced crystal damage, achieving higher-brightness ensembles. 1 MeV proton irradiation with  $10^{13} \text{ cm}^{-2}$  at 200 °C could achieve a 2–3 times stronger photoluminescence intensity enhancement than that at room-temperature irradiation. We established a controllable fabrication methodology for engineering the brightness of color-center ensembles through precise tuning of irradiation conditions, which paves the foundation for fabricating high-quality  $V_{Si}^-$  color-center ensembles and other color-center systems in wide-bandgap semiconductor materials.

Published under an exclusive license by AIP Publishing. <https://doi.org/10.1063/5.0288542>

Quantum sensing based on color-center systems<sup>1</sup> is one of the most promising technical approaches in quantum technology. Color centers are unique solid-state spin defects in materials, and these solid-state spin systems in wide-bandgap semiconductor materials have emerged as critical platforms for quantum information science and precision metrology. The silicon vacancy ( $V_{Si}^-$ ) color center in 4H-SiC is one of the current representative systems. First, the  $V_{Si}^-$  color center can maintain quantum properties at room temperature with long relaxation and spin coherence time,<sup>2</sup> which allows sophisticated quantum manipulations. Moreover, the spin states of  $V_{Si}^-$  centers can be optically manipulated and read out through their controllable spin–photon interface. Meanwhile, the fluorescence, including the zero-photon line (ZPL) of  $V_{Si}^-$  centers, lies in the near-infrared region. Furthermore, the single spin orientation of  $V_{Si}^-$  centers in 4H-SiC<sup>3,4</sup> along the crystallographic c-axis, as well as the mature semiconductor fabrication techniques compatible with silicon carbide, enable the  $V_{Si}^-$  color centers'

distinct advantages for quantum sensing. Indeed,  $V_{Si}^-$ -center-based quantum sensing has drawn much attention from research groups and industries worldwide.

The quality of color-center ensembles is a vital factor influencing the performance of quantum sensing. Currently, the fabrication of vacancy-related color centers, such as the  $V_{Si}^-$  centers in 4H-SiC, is mainly achieved through energetic particle irradiation. The irradiation methods in most research include high-energy electrons,<sup>3,5</sup> neutrons,<sup>6</sup> and ion irradiation,<sup>7,8</sup> in which MeV electrons are the most common irradiation type used. Ideal color-center ensembles should meet the requirement of high brightness for effective optically detected magnetic resonance (ODMR) signal measurements.<sup>2,9</sup> However, high-energy electron or neutron irradiation could penetrate the whole host material, leading to the defect depth profiles of the ensembles typically extending beyond several hundred micrometers. These color centers deep inside the material are difficult to utilize, constraining effective enhancement of the brightness of ensembles.

Ion irradiation offers distinct advantages for fabricating color-center defects due to its capability of precise irradiation depth via adaptation of irradiation parameters. Theoretically, ion irradiation could realize the three-dimensional high-resolution introduction of the color center into the host matrix with atomic-level precision and fulfill the demand for the fabrication of large uniform, bulk samples of color centers as well.<sup>6,10</sup> By tuning irradiation parameters such as ion energy and species, color centers can be controlled within the desired depth,<sup>11</sup> effectively preventing the formation of color centers and other spin defects deep inside the host material. However, the production yield of color centers remains considerably low at the current stage. Energetic ion tends to generate a higher density of defects. The undesired other defects and lattice damage introduced during irradiation significantly hinder the realization of high-brightness samples with a single type of color center.<sup>12</sup> Consequently, the impact of the displacement damage in the host material of irradiation on the brightness of color-center ensembles should be systematically investigated.

Creating color-center ensembles via ion irradiation exhibits a stronger dependence on post-annealing processes to facilitate defect conversion and lattice recovery, resulting in a significant thermal budget requirement. Meanwhile, high fluence or heavier ion irradiation typically demands elevated annealing temperatures for effective damage recovery and the formation of the targeted color center.<sup>8</sup> Several studies indicate that irradiation at specific high temperatures can reduce the thermal budget requirement for subsequent annealing processes, enhancing the production yield of NV centers in diamond.<sup>13</sup> However, this approach lacks experimental validation for other color-center systems, such as  $V_{Si}^-$  centers in 4H-SiC.

In this work, we conducted systematic irradiation experiments using MeV electrons, protons, and laser-driven ions to fabricate high-brightness  $V_{Si}^-$  color-center ensembles and investigate the influence of irradiation parameters upon the brightness of  $V_{Si}^-$  center ensembles. We confirmed the critical impact of the displacement damage density of different irradiations on the production yield of  $V_{Si}^-$  centers. To further elucidate the irradiation temperature on the production yield of  $V_{Si}^-$  centers, the hot irradiation experiments were performed subsequently, which demonstrates that the optimized irradiation temperature conditions can overcome the inherent limitation of the radiation-induced crystal damage, achieving a significantly higher production rate of  $V_{Si}^-$  centers compared to room-temperature (RT) irradiation. Our results pave a clear path toward developing high-brightness color-center ensembles for a broad range of quantum applications.

The host material adopted was high-purity semi-insulating (HPSI) 4H-SiC substrates (Si-face CMP) with an orientation of  $\langle 0001 \rangle \pm 0.5^\circ$  from the Shanghai Institute of Optics and Fine Mechanics, possessing a resistivity larger than  $10^5 \Omega \text{ cm}$ . After laser-dicing into  $3 \times 3 \text{ mm}^2$  chips, these 4H-SiC samples were first ultrasonically washed in Piranha acid ( $\text{H}_2\text{SO}_4\text{:H}_2\text{O}_2 = 3\text{:}1$ ) for 1 h to remove surface contaminants. Thermal treatment under vacuum was further used to remove the existing defects in all experimental specimens, which ensured sample uniformity. The annealing procedure was performed using the SK-G06143 tube annealing furnace, with sequential 3 h dwells at 900 and 1100 °C, maintaining a vacuum level of approximately  $10^{-4} \text{ Pa}$  throughout the process. Finally, an ion etching process (500 eV  $\text{Ar}^+$ ) was employed to remove surface oxide layers formed during wet chemical cleaning and pre-annealing treatments. The photoluminescence (PL) results shown in Figs. S1(a) and S1(b) of the

supplementary material demonstrate that the pre-annealing process effectively eliminates the majority of defects in the material, including  $V_{Si}^-$  centers, thereby achieving great homogeneity between different samples. The x-ray photoelectron spectroscopy (XPS) results in Figs. S1(c) and S1(d) indicate that ion etching effectively removes surface oxide layers, while the confocal photoluminescence (PL) measurements in Figs. S1(e) and S1(f) confirm negligible defect introduction into the bulk material from the 500 eV  $\text{Ar}^+$  etching, as detailed in the supplementary material.

Following the pre-treatment procedure, the samples were irradiated to introduce  $V_{Si}^-$  centers into the host material. The irradiation experiments were conducted using several accelerator facilities at the State Key Laboratory of Nuclear Physics and Technology, Peking University, including (a)  $2 \times 1.7 \text{ MV}$  tandem accelerator,<sup>14</sup> (b) DC-SRF-II photocathode gun,<sup>15</sup> and (c) the Compact Laser Plasma Accelerator (CLAPA) facility.<sup>16</sup> The detailed irradiation parameters are summarized in Table I. First, we conducted the irradiation experiment with varying fluences at room temperature, including 2 MeV electron irradiation experiments ( $10^{14}\text{--}10^{18} \text{ cm}^{-2}$ ) at the DC-SRF-II platform, and 1 MeV proton irradiation experiments ( $10^{11}\text{--}10^{15} \text{ cm}^{-2}$ ) at the  $2 \times 1.7 \text{ MV}$  tandem accelerator. The laser-accelerated ion irradiation experiments were performed using the CLAPA facility, and the laser-driven ion energy spectrum is shown in Fig. S2. Accordingly, we selected fluences of  $10^{13}$  and  $10^{14} \text{ cm}^{-2}$  to conduct 1 MeV proton irradiation experiments at elevated temperatures (200–800 °C). During the experiments, the samples were first heated to the targeted temperature, and then irradiation experiments with fluences of  $10^{14}$  and  $10^{13} \text{ cm}^{-2}$  were sequentially carried out to minimize the influence of high temperature after irradiation on these samples. After the irradiation was completed, the heat source was immediately turned off, and then the samples were cooled in the furnace, while the temperature was monitored until it dropped below 200 °C. The cooling curve is shown in Fig. S3. The irradiation incident directions adopted in this work were all  $[000 \bar{1}]$ . Except for the laser-driven ion irradiation experiment with the fluence of  $10^{10} \text{ cm}^{-2}$  and the electron irradiation experiments (where only one sample was used), all other parameter sets employed three samples to ensure statistical reliability.

Photoluminescence (PL) was measured using an FLS980 spectrometer, with a 785 nm excitation laser from CNI Optoelectronics Technology Co., Ltd. Two 830 nm long-pass filters were utilized to eliminate reflected laser interference in the spectrum. Furthermore, between the measurements of different samples, the laser power and instrument setup remained constant, while neutral density (ND) filters were employed to adjust the fluorescence intensity within the optimal detection range of the FLS980 spectrometer. The acquired PL spectra were subsequently corrected based on the transmission spectra of the

TABLE I. 4H-SiC samples and irradiation conditions used in this study.

Sample	Irradiation type	Fluence	Irradiation temperature
HPSI 4H-SiC	2 MeV $e^-$	$10^{14}\text{--}10^{18} \text{ cm}^{-2}$	RT
HPSI 4H-SiC	1 MeV proton	$10^{11}\text{--}10^{15} \text{ cm}^{-2}$	RT, 200, 400, 600, 800 °C
HPSI 4H-SiC	Laser-driven ions	$\sim 10^9, 10^{10} \text{ cm}^{-2}$	RT

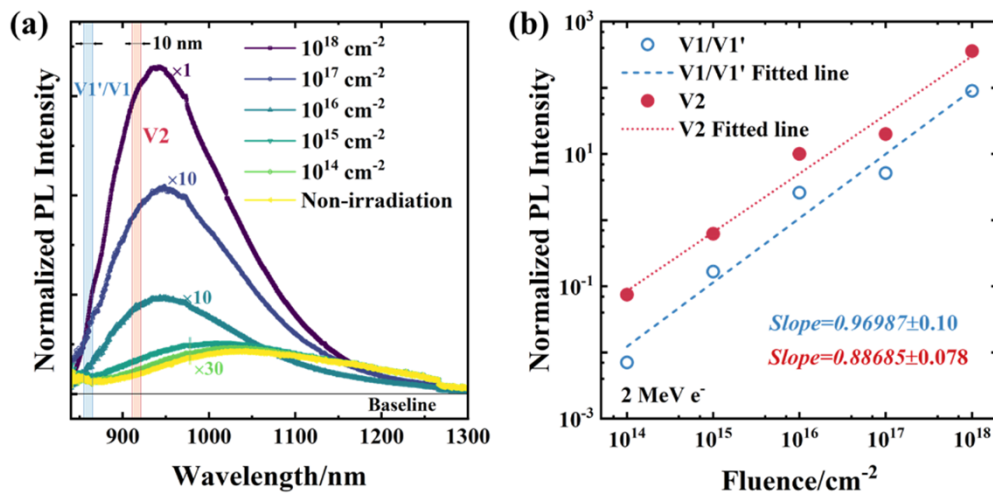


**FIG. 1.** Fabrication of  $V_{Si}^-$  color-center ensembles via 2 MeV electron irradiation. (a) PL spectra of  $V_{Si}^-$  color-center ensembles under different fluences acquired at RT. (b) Normalized PL intensity vs 2 MeV electron irradiation fluence.

corresponding ND filters to reconstruct the unattenuated PL spectra. The transmission spectra of the neutral density (ND) filters were measured using a UV3600Plus spectrophotometer.

Figure 1(a) shows the PL spectra acquired at RT of  $V_{Si}^-$  center ensembles under different fluences of 2 MeV electron irradiation, and Fig. S4 presents the low-temperature (LT) PL spectra of  $V_{Si}^-$  center ensembles fabricated via 2 MeV electron irradiation with a fluence of  $10^{18}$  cm $^{-2}$ . The zero-phonon lines (ZPL) of V1'/V1 (h) centers are located at 857.5 and 860 nm, while the ZPL of V2 (k) centers appears at 914.5 nm, which is consistent with previous reports.<sup>3</sup> Meanwhile, we confirm the formation of  $V_{Si}^-$  centers in the irradiated samples using our home-built optically detected magnetic resonance (ODMR) system, as demonstrated in Fig. S5.

With increasing fluence of electron irradiation, the contribution of both the ZPL and their phonon sidebands from  $V_{Si}^-$  centers becomes significantly enhanced in the PL spectra. At fluences above  $10^{16}$  cm $^{-2}$ , the fluorescence within 850–1000 nm dominates the spectra profile, indicating that  $V_{Si}^-$  centers constitute the majority of defects in the host material. Based on the ZPL positions identified from the LT PL spectra of  $V_{Si}^-$  centers in Fig. S4, a 10 nm wavelength range was selected for spectral integration of the data in Fig. 1(a). The integrated intensities were, respectively, assigned to V1 and V2 centers, and the normalized results are presented in Fig. 1(b). The PL intensities of both V1 and V2 centers exhibit similar increasing trends as increasing electron irradiation fluence. The results of log-linear regression fitting (power-law fitting,  $I_{PL} = Cx^\alpha$ ) are shown as dashed lines in Fig. 1(b). For the V1 centers, the obtained power-law exponent  $\alpha = 0.97 \pm 0.1$  indicates an approximately linear increase in V2 center concentration with fluence under 2 MeV electron irradiation. This result agrees well with literature reports, demonstrating that the PL intensity of  $V_{Si}^-$  centers maintains linear growth even at a high fluence of  $10^{19}$  cm $^{-2}$  under 2 MeV electron irradiation<sup>17</sup> and exhibits no saturation behavior.

Figure 2(a) shows the PL spectra acquired at RT of  $V_{Si}^-$  center ensembles under different fluences of 1 MeV proton irradiation, and Fig. 2(b) presents the integrated PL intensities of V1/V2 centers

obtained at different fluences, along with their corresponding log-linear regression fitting curves. The power-law exponent  $\alpha$  of the fitting curves of V1 centers is  $0.829 \pm 0.095$ , suggesting that the generation rate of V1 centers slows down with the increase in 1 MeV proton fluence. We attributed the constraining of the  $V_{Si}^-$  centers formation to the accumulation of radiation-induced lattice damage as the fluence increases. It is worth noting that the fitting power exponents of V2 color centers in the 2 MeV electron irradiation experiment and the 1 MeV proton irradiation experiment are both slightly smaller than those of V1 color centers. The increase in fluence has different effects on the generation rates of  $V_{Si}^-$  centers at two different sites. Several research works<sup>18,19</sup> show the kinetic energy of atoms displaced by MeV-electron irradiation is comparable to the threshold displacement energies (TDE) of Si/C atoms in silicon carbide. Furthermore, while the minimum displacement threshold energies for silicon atoms at different lattice sites in 4H-SiC are comparable, they exhibit significantly different directional dependencies.<sup>19</sup> Along the  $[000\bar{1}]$  direction, the TDE for Si atoms at cubic (k) sites is considerably higher than that of hexagonal (h) sites. Under the same energy transfer condition, we infer that the more pronounced local lattice distortion around k sites hinders the formation of V2 centers. Consequently, the production rate of V2 centers slows down with increasing fluence.

Figure 3(a) compares the normalized PL intensity of  $V_{Si}^-$  center ensembles fabricated by 2 MeV electron irradiation and proton irradiation. The  $V_{Si}^-$  center ensembles produced via 1 MeV proton irradiation with a fluence of  $10^{14}$  cm $^{-2}$  exhibit comparable brightness to the ensembles under 2 MeV electron irradiation of  $10^{17}$  cm $^{-2}$ . To investigate the influence of displacement damage in SiC of different irradiations upon the brightness of ensembles, Fig. S6(a) presents the total number of vacancies generated in silicon carbide of different energetic particles below 10 MeV. While the total vacancies introduced into SiC increase with particle energy for all incident species, the average vacancy density along the depth decreases with particle energy for most particles in Fig. S6(b). According to the results in Fig. S6(b), Fig. 3(b) shows the normalized PL intensity of  $V_{Si}^-$  center ensembles as a function of displacement damage density with different irradiation

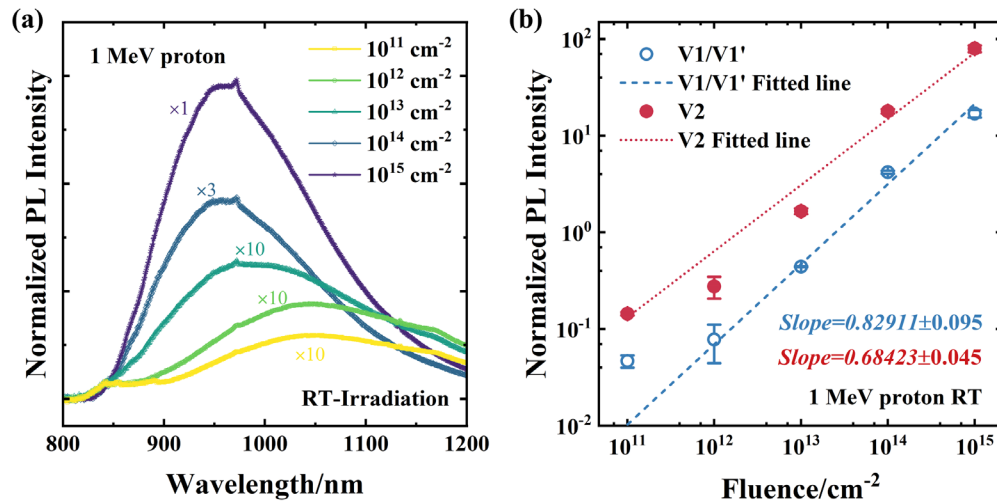


**FIG. 2.** Fabrication of  $V_{Si}^-$  color-center ensembles via 1 MeV proton irradiation. (a) PL spectra of  $V_{Si}^-$  color-center ensembles under different proton fluences acquired at RT. (b) Normalized PL intensity vs 1 MeV proton irradiation fluence.

parameters. Under equal displacement damage, 1 MeV protons could generate  $V_{Si}^-$  center ensembles with higher brightness than 2 MeV electron irradiation. However, the fitting power-law exponent of 1 MeV proton irradiation experiments is less than that of 2 MeV electron irradiation experiments, indicating that the  $V_{Si}^-$  centers per proton of 1 MeV decrease faster than that of 2 MeV electron irradiation as the fluence increases.

Consequently, we conclude that the observed divergence in  $V_{Si}^-$  centers' production yield stems primarily from radiation-type-dependent crystal damage densities, which further constrain the achievable color-center concentrations through increasing irradiation fluence. Figure S6(b) reveals that heavier particles could create a denser vacancy profile along the depth and higher displacement damage density with the same energy. At low fluences ( $\leq 10^{12}$  cm $^{-2}$ ), crystal

damage is governed by individual particle energy and mass. However, in the high-fluence regime, despite their lower displacement damage compared to protons, MeV electrons ultimately produce less cumulative lattice disorder, thereby enabling the generation of brighter color-center ensembles through fluence escalation. Moreover, by comparing the ratio of the PL intensity between V1 and V2 color centers under different irradiation parameters, we infer that the irradiation types exhibit small effects on the relative formation efficiency between V1 and V2 centers. Figure 3 also presents the normalized results of ensembles by laser-driven ions. The fluence of a single-shot at the sample position<sup>16</sup> was approximately  $10^9$  cm $^{-2}$ . While MeV carbon ions generate only  $\sim 10^2$  times more vacancies than 1 MeV protons in SiC, the ensembles by laser-driven ions with  $\sim 10^{10}$  cm $^{-2}$  could have superior brightness compared to that of 1 MeV proton irradiation with

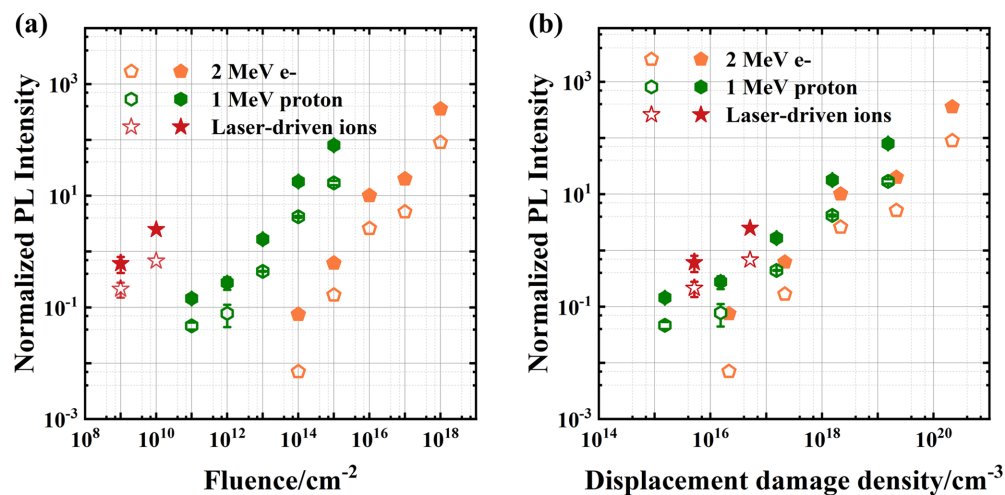


**FIG. 3.** Normalized PL intensity of  $V_{Si}^-$  center ensembles as a function of fluence (a) and displacement damage density (b) under different irradiation parameters. Open symbols denote V1/V1' centers, while solid symbols represent V2 centers.



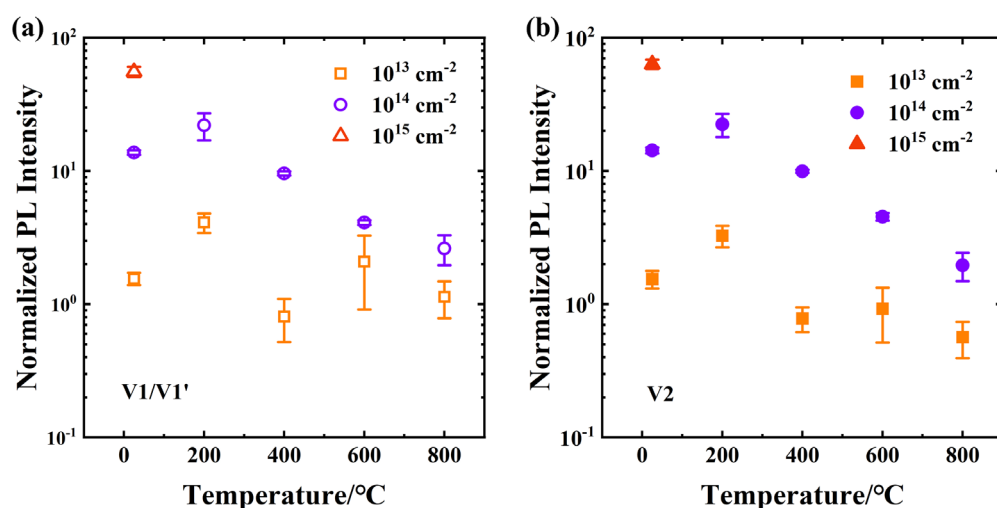


FIG. 4. The normalized PL intensity of V1 (a) and V2 (b) center ensembles by 1 MeV protons under different irradiation temperatures.

$10^{13} \text{ cm}^{-2}$ . We attribute this anomalous enhancement in  $V_{\text{Si}}^-$  centers' formation efficiency to the transient localized spatiotemporal temperature profile induced by laser-accelerated ions in SiC, where transient localized heating may promote the conversion to desired  $V_{\text{Si}}^-$  centers.<sup>20</sup>

To further elucidate the influence of sample temperature during irradiation on the formation of  $V_{\text{Si}}^-$  center ensembles, we performed the 1 MeV proton experiments at fluences of  $10^{13}$  and  $10^{14} \text{ cm}^{-2}$  under different irradiation temperature range from 200 to 800 °C. The PL spectra of  $V_{\text{Si}}^-$  center ensembles under different irradiation temperatures are shown in Fig. S8. The PL spectral profiles of the ensembles obtained under different irradiation temperatures all match those of the high-fluence electron-irradiated samples, demonstrating the dominant presence of  $V_{\text{Si}}^-$  centers in these samples. Figure 4 presents the normalized PL intensities of V1/V2 centers by 1 MeV protons under different irradiation temperatures. The results reveal that 1 MeV proton irradiation at 200 °C produces the highest-brightness ensembles among all 1 MeV proton irradiation groups, indicating a significant irradiation temperature dependence of  $V_{\text{Si}}^-$  center ensembles, with 200 °C proton irradiation ( $10^{13} \text{ cm}^{-2}$ ) yielding 2–3-fold enhancement in PL intensity compared to RT irradiation. Irradiation at optimized temperatures could enhance the production yield of  $V_{\text{Si}}^-$  centers and break the inherent limitation of radiation-induced crystal damage, achieving higher-brightness ensembles. Compared to the  $10^{14} \text{ cm}^{-2}$  fluence, lower-fluence irradiation at 200 °C exhibits a more significant enhancement in color-center brightness. We attribute this observation to the possible requirement of adjusted irradiation temperatures for higher fluences. Notably, when the irradiation temperature exceeds 400 °C, the PL intensity of the obtained  $V_{\text{Si}}^-$  center ensembles decreases remarkably, indicating reduced radiation damage of 1 MeV protons in 4H-SiC at elevated irradiation temperatures.

In summary, we performed irradiation experiments of MeV electrons, protons, and laser-driven ions to fabricate the  $V_{\text{Si}}^-$  center ensembles, investigating the difference between different irradiations upon production of the  $V_{\text{Si}}^-$  center ensembles. The observed divergence

in  $V_{\text{Si}}^-$  centers production yield under different irradiations stems primarily from radiation-type-dependent crystal damage densities, which further constrain the achievable color-center concentrations through increasing irradiation fluence. Although individual 1 MeV protons could generate more  $V_{\text{Si}}^-$  centers than 2 MeV electrons, their cumulative displacement damage at higher fluences ultimately limits  $V_{\text{Si}}^-$  centers production, resulting in the slow-down growth of PL intensity with increasing fluence. Meanwhile, the irradiation types exhibit little effects on the relative formation efficiency between V1 and V2 centers in 4H-SiC. Furthermore, we infer that the transient localized heating induced by laser-driven ions in SiC enhanced the production of  $V_{\text{Si}}^-$  centers. Meanwhile, the hot irradiation experiments demonstrate that irradiation at optimized temperatures could enhance the production yield of  $V_{\text{Si}}^-$  centers and break the inherent limitation of radiation-induced crystal damage, achieving higher-brightness ensembles. 1 MeV proton irradiation with  $10^{13} \text{ cm}^{-2}$  at 200 °C could achieve a 2–3 times stronger PL intensity enhancement than that at room-temperature irradiation. The methodology developed in this work can be generalized to engineer other solid-state spin defects in wide-bandgap semiconductors, paving the foundation to fabricate high-quality color-center ensembles.

See the [supplementary material](#) for the experimental details of sample pretreatment and irradiation (Secs. 1 and 2), the identification of the  $V_{\text{Si}}^-$  center in 4H-SiC (Sec. 3), SRIM calculation details for displacement damage of ions in SiC (Sec. 4), and the room-temperature photoluminescence spectrum of samples after high-temperature irradiation (Sec. 5).

This work was supported by the National Natural Science Foundation of China (Grant No. 12135002).

## AUTHOR DECLARATIONS

### Conflict of Interest

The authors have no conflicts to disclose.

## Author Contributions

**Shang Tian:** Conceptualization (equal); Data curation (equal); Formal analysis (equal); Investigation (equal); Methodology (equal); Validation (equal); Visualization (equal); Writing – original draft (equal); Writing – review & editing (equal). **Huaqing Huang:** Formal analysis (equal); Writing – review & editing (equal). **Haozheng Guo:** Data curation (equal); Writing – review & editing (equal). **Jianhan Sun:** Methodology (equal); Writing – review & editing (equal). **Yulan Liang:** Methodology (equal); Writing – review & editing (equal). **Yewei Song:** Methodology (equal); Writing – review & editing (equal). **Yunbiao Zhao:** Investigation (equal); Supervision (equal); Writing – review & editing (equal). **Yuan Gao:** Investigation (equal); Supervision (equal); Writing – review & editing (equal). **Lin Lin:** Investigation (equal); Methodology (equal). **Senlin Huang:** Resources (equal); Supervision (equal). **Wenjun Ma:** Resources (equal); Supervision (equal). **Jianming Xue:** Conceptualization (equal); Funding acquisition (equal); Investigation (equal); Methodology (equal); Project administration (equal); Resources (equal); Supervision (equal); Writing – review & editing (equal).

## DATA AVAILABILITY

The data that support the findings of this study are available from the corresponding author upon reasonable request.

## REFERENCES

- <sup>1</sup>H. Guo, T. Wu, B. Luo, and Y. X. Liu, *Physics* **53**(6), 384 (2024); C. L. Degen, F. Reinhard, and P. Cappellaro, *Rev. Mod. Phys.* **89**(3), 035002 (2017).
- <sup>2</sup>G. Wolfowicz, F. J. Heremans, C. P. Anderson, S. Kanai, H. Seo, A. Gali, G. Galli, and D. D. Awschalom, *Nat. Rev. Mater.* **6**(10), 906 (2021).
- <sup>3</sup>S. Castelletto and A. Boretti, *J. Phys.: Photonics* **2**(2), 022001 (2020).
- <sup>4</sup>V. A. Soltamov, B. V. Yavkin, D. O. Tolmachev, R. A. Babunts, A. G. Badalyan, V. Y. Davydov, E. N. Mokhov, I. I. Proskuryakov, S. B. Orlinskii, and P. G. Baranov, *Phys. Rev. Lett.* **115**(24), 247602 (2015).
- <sup>5</sup>M. Widmann, S. Y. Lee, T. Rendler, N. T. Son, H. Fedder, S. Paik, L. P. Yang, N. Zhao, S. Yang, I. Booker, A. Denisenko, M. Jamali, S. A. Momenzadeh, I. Gerhardt, T. Ohshima, A. Gali, E. Jánzén, and J. Wrachtrup, *Nat. Mater.* **14**(2), 164 (2015); R. Nagy, M. Niethammer, M. Widmann, Y. C. Chen, P. Udvarhelyi, C. Bonato, J. U. Hassan, R. Karhu, I. G. Ivanov, N. T. Son, J. R. Maze, T. Ohshima, O. O. Soykal, A. Gali, S. Y. Lee, F. Kaiser, and J. Wrachtrup, *Nat. Commun.* **10**(1), 1954 (2019); C. P. Anderson, E. O. Glen, C. Zeledon, A. Bourassa, Y. Jin, Y. Zhu, C. Vorwerk, A. L. Crook, H. Abe, J. Ul-Hassan, T. Ohshima, N. T. Son, G. Galli, and D. D. Awschalom, *Sci. Adv.* **8**(5), eabm5912 (2022).
- <sup>6</sup>C. Kasper, D. Klenkert, Z. Shang, D. Simin, A. Gottscholl, A. Sperlich, H. Kraus, C. Schneider, S. Zhou, M. Trupke, W. Kada, T. Ohshima, V. Dyakonov, and G. V. Astakhov, *Phys. Rev. Appl.* **13**(4), 044054 (2020).
- <sup>7</sup>S. Ernst, P. J. Scheidegger, S. Diesch, L. Lorenzelli, and C. L. Degen, *Phys. Rev. Lett.* **131**(8), 086903 (2023); D. M. Lukin, C. Dory, M. A. Guidry, K. Y. Yang, S. D. Mishra, R. Trivedi, M. Radulaski, S. Sun, D. Vercruysse, G. H. Ahn, and J. Vučković, *Nat. Photonics* **14**(5), 330 (2020).
- <sup>8</sup>J. F. Wang, Q. Li, F. F. Yan, H. Liu, G. P. Guo, W. P. Zhang, X. Zhou, L. P. Guo, Z. H. Lin, J. M. Cui, X. Y. Xu, J. S. Xu, C. F. Li, and G. C. Guo, *ACS Photonics* **6**(7), 1736 (2019).
- <sup>9</sup>Z. Mu, S. A. Zargaleh, H. J. von Bardeleben, J. E. Fröch, M. Nonahal, H. B. Cai, X. G. Yang, J. Q. Yang, X. J. Li, I. Aharonovich, and W. B. Gao, *Nano Lett.* **20**(8), 6142 (2020).
- <sup>10</sup>R. Karsthof, M. E. Batten, A. Galeckas, and L. Vines, *Phys. Rev. B* **102**(18), 184111 (2020).
- <sup>11</sup>T. Z. Sun, Z. W. Xu, J. T. Wu, Y. X. Fan, F. Ren, Y. Song, L. Yang, and P. H. Tan, *Ceram. Int.* **49**(5), 7452 (2023).
- <sup>12</sup>J. F. Barry, J. M. Schloss, E. Bauch, M. J. Turner, C. A. Hart, L. M. Pham, and R. L. Walsworth, *Rev. Mod. Phys.* **92**(1), 015004 (2020); M. Rühl, C. Ott, S. Götzinger, M. Krieger, and H. B. Weber, *Appl. Phys. Lett.* **113**(12), 122102 (2018).
- <sup>13</sup>M. W. Ngandeu Ngambou, P. Perrin, I. Balasa, A. Tiranov, O. Brinza, F. Bénédict, J. Renaud, M. Reveillard, J. Silvent, P. Goldner, J. Achard, and A. Tallaie, *Appl. Phys. Lett.* **124**(13), 134002 (2024); M. Capelli, A. H. Heffernan, T. Ohshima, H. Abe, J. Jeske, A. Hope, A. D. Greentree, P. Reineck, and B. C. Gibson, *Carbon* **143**, 714 (2019).
- <sup>14</sup>C. Xu and E. G. Fu, *Nucl. Phys. Rev.* **38**(4), 410 (2021).
- <sup>15</sup>S. L. Huang, K. X. Liu, K. Zhao, and J. E. Chen, *Chin. Sci. Bull.* **68**(9), 1036 (2023); J. H. Sun, J. F. Lv, S. Tian, J. T. Liu, Z. H. Zhang, H. Xu, L. Lin, and S. L. Huang, *Phys. Scr.* **100**(6), 065010 (2025).
- <sup>16</sup>Z. P. Liu, Y. Gao, Q. F. Wu, Z. Pan, Y. L. Liang, T. Song, T. Q. Xu, Y. R. Shou, Y. J. Zhang, H. R. Chen, Q. H. Han, C. H. Hua, X. Chen, S. R. Xu, Z. S. Mei, P. J. Wang, Z. Y. Peng, J. R. Zhao, S. Y. Chen, Y. Y. Zhao, X. Q. Yan, and W. J. Ma, *Phys. Plasmas* **31**(5), 053106 (2024).
- <sup>17</sup>S. Motoki, S.-I. Sato, S. Saiki, Y. Masuyama, Y. Yamazaki, T. Ohshima, K. Murata, H. Tsuchida, and Y. Hijikata, *J. Appl. Phys.* **133**(15), 154402 (2023).
- <sup>18</sup>A. A. Rempel, W. Sprengel, K. Blaurock, K. J. Reichle, J. Major, and H. E. Schaefer, *Phys. Rev. Lett.* **89**(18), 185501 (2002).
- <sup>19</sup>W. Liu, P. S. Guo, Z. Y. Zheng, S. Y. Chen, and Y. N. Wu, *Adv. Electron. Mater.* **11**(11), 2400911 (2025).
- <sup>20</sup>W. Redjem, A. J. Amsellem, F. I. Allen, G. Benndorf, J. Bin, S. Bulanov, E. Esarey, L. C. Feldman, J. Ferrer Fernandez, J. G. Lopez, L. Geulig, C. R. Geddes, H. Hijazi, Q. Ji, V. Ivanov, B. Kanté, A. Gonsalves, J. Meijer, K. Nakamura, A. Persaud, I. Pong, L. Obst-Huebl, P. A. Seidl, J. Simoni, C. Schroeder, S. Steinke, L. Z. Tan, R. Wunderlich, B. Wynne, and T. Schenkel, *Commun. Mater.* **4**(1), 22 (2023).